This paper is a postprint of a paper submitted to and accepted for publication in *IET Electric Power Applications* and is subject to Institution of Engineering and Technology Copyright. The copy of record is available at IET Digital Library

A Condition Monitoring Approach for PMSM Drives based on the INFORM Method

J. Arellano-Padilla[1], M. Sumner[2], C. Gerada[3]

Department of Electrical and Electronic Engineering

University of Nottingham; Nottingham, UK

jesus.arellano@nottingham.ac.uk[1]; mark.sumner@nottingham.ac.uk[2]; chris.gerada@nottingham.ac.uk[2]

***Abstract*—**This paper proposes a monitoring scheme based on saliency tracking to assess the health condition of PMSM drives operating under non stationary conditions. The evaluated scheme is based on the INFORM methodology, which is associated to the accurate sensorless control of PM drives without zero speed limitation. The result is a monitoring scheme that is able to detect faults that would be very difficult to evaluate under nonstationary conditions. A relevant aspect of the proposed scheme is that it remains valid for full speed range, and can be used for standstill operation. Additionally, the approach is insensitive to the inverter nonlinearities which enhance the detection capabilities further respect to similar topologies.

In this work the proposed approach is evaluated numerically and experimentally in the presence of incipient winding faults and inter-turn short circuits in a PM conventional drive. The obtained results show quick response and excellent detection capabilities not only in the detection of faults, but to determine their magnitude which is vital to avoid further degradation.

I. INTRODUCTION

One of the most critical components in motor drives is the stator winding insulation. Recent surveys on motor reliability show that the percentage of motor failures due to problems with the insulation system is in the range of 26-36% [1-3]. In most cases deterioration begins with the appearance of an inter-turn fault, where two or more turns become short circuited [4]. At this stage, little can be observed externally, however currents in the affected turns may be substantially higher than the operational current which is determined by the rotor speed. Inter-turn faults may develop into severe failures if left unattended. Several schemes aimed to the detection of winding faults can be found in literature [5]: *Offline-methods* are direct and accurate [4], however the required tests can only be performed to motors that are disconnected from service, which is undesirable. *Online-monitoring* on the other hand is preferred since the health condition can be assessed while the machine is in operation.

Conventional online-monitoring includes temperature tracking, measurement of sequence components, and signature analysis. Temperature monitoring [6] requires temperature sensors embedded within the stator windings and the machine's frame. Detection of inter-turn faults at early stage of development seems unlikely unless the embedded sensor is located very close to the affected area (hot spot) which is unlikely. Other schemes are based on the measurement of the sequence components of the machine's impedance [7], currents [8], or voltages [9]. These schemes have proven to be very successful for the detection of winding faults in motors connected to the grid (mainly induction motors); however performance degrades considerably for motors supplied by a power converters, this due to the inverter nonlinearities [10]. Other methods based on signature

analysis have been suggested as alternatives to detect winding faults, this assuming that new harmonic frequencies are created in the presence of faults. The more representative schemes are based on current [11], vibration [12], and axial leakage flux [13] measurements. Note that signature analysis requires extraction of the harmonic components of a monitored variable, which is usually obtained by FFT methods; which means that these solutions are not always suitable for drives operating under nonstationary conditions or position holding applications. An additional problem is that it is not always possible to discriminate between harmonics related to specific faults from those related to other sources (motor asymmetries, load disturbances or unbalanced supply).

Some solutions to deal with these problems are based on pattern recognition techniques, and wavelets. For instance, in [14] an approach based on complex gauss wavelets applied to the instantaneous power is proposed. The scheme is able to deal with no stationary conditions however is not suitable for standstill operation.

Other advanced schemes aimed to the detection of faults in drives operating under nonstationary conditions have been proposed; for instance in [15] an approach based on an extended Kalman filter shows a quick response and excellent detection capabilities in the presence of inter-turn winding faults. Unfortunately the scheme is not suitable for standstill operation. Other schemes propose the use of a high-frequency (HF) signal injection. This is the case of [16], where a carrier signal is added to monitor aging and deterioration of winding insulation by detecting changes in the turn-to-turn capacitance. The resulting flux is measured by a magnetic probe where changes in the phase lag are used to estimate changes in the insulation. A main problem is that the frequency of the injected signal should be close to the machine's resonance frequency (several MHz) which may require external HF sources which makes the method impractical. Other schemes based on HF signal injection use saliency tracking (saliency-based condition monitoring) as those reported in [17-18]. In [17] the resulting high-frequency negative-sequence measured from the machine currents are used to detect winding faults and rotor broken bars in induction machines. This is relevant since sequence measurement methods which were initially restricted for line-fed machines, can be used. The scheme has the potential to be used for standstill operation; however requires FFT to improve the resolution capability in the presence of incipient faults.

A different approach based on HF injection was developed by these authors and reported in [18]. This scheme combined saliency tracking (based on HF injection [19]), and Saliency Modulation Profiling (SMP) [20-21] to improve the detection capabilities. The approach showed excellent performance, however was only suitable for medium to low speed applications, this due to the maximum carrier frequency that can be applied to a discrete system is considerably limited. The monitoring scheme presented in this paper is an improved version of [18], however in this case saliency tracking is based on the INFORM methodology [22-24] which has no speed range limitations. Another advantage is that the scheme is not affected by the inverter nonlinearities [10]; this improves the detection capabilities further respect to that reported in [18]. In this paper the proposed scheme will be evaluated numerically and experimentally for the presence of incipient winding faults and inter-turn short circuits in a PM drive.

Organisation of the paper is as follows: Section II introduces the PWM transient excitation scheme; the SMP concept aimed to improve sensibility and to extend operation for standstill conditions is briefly explained in Section III; Section IV contains simulation and experimental validation for the case several windings faults in a PMSM drive. Final remarks and Conclusions are included in Section V.

II. PWM TRANSIENT EXCITATION SCHEME

The tracking of anisotropic properties of the rotor by the leakage inductance modulations has become a standard mechanism for rotor position estimation in AC drives without restriction of zero frequency [19]. Two basic schemes associated to saliency tracking can be found in literature: High frequency (HF) signal injection [25], and PWM transient excitation [22-24]. The monitoring scheme proposed in this paper is based on the latter. Several schemes for PWM transient excitation have been proposed, however all of them are derived from an approach referred as "indirect flux detection by on-line reactance measurement methodology", or simply as INFORM [23]. This scheme is briefly described in this Section.

Considering the effects of saliency modulation due to the rotor anisotropies [26], the phase leakage inductances of a PMSM machine can be expressed as:

$$\begin{aligned} l_{\sigma a} &= l_0 + \Delta l \cos(2\theta_{an}) \\ l_{\sigma b} &= l_0 + \Delta l \cos\big(2(\theta_{an} - 2\pi/3)\big) \\ l_{\sigma c} &= l_0 + \Delta l \cos\big(2(\theta_{an} - 4\pi/3)\big) \end{aligned} \tag{1}$$

where $l_{\sigma abc}$ are the phase leakage inductances, l_0 is the average inductance, and Δl is the maximum inductance variation according to the saliency angle θ_{an} determined by the rotor anisotropy (spatial saliency). The INFORM method decomposes the reference voltage vector (u_{ref}) into basic vectors realizable by a three-phase inverter; this according to a SVPWM topology [27]. This procedure is shown in Fig.1a, where the basic PWM vectors are separated into six switching sectors (numbered by *I, II,…VI*), while the basic vectors (V_1 …V_6) are represented by six active switching states. The inactive states (null vectors) are V_0 and V_7.

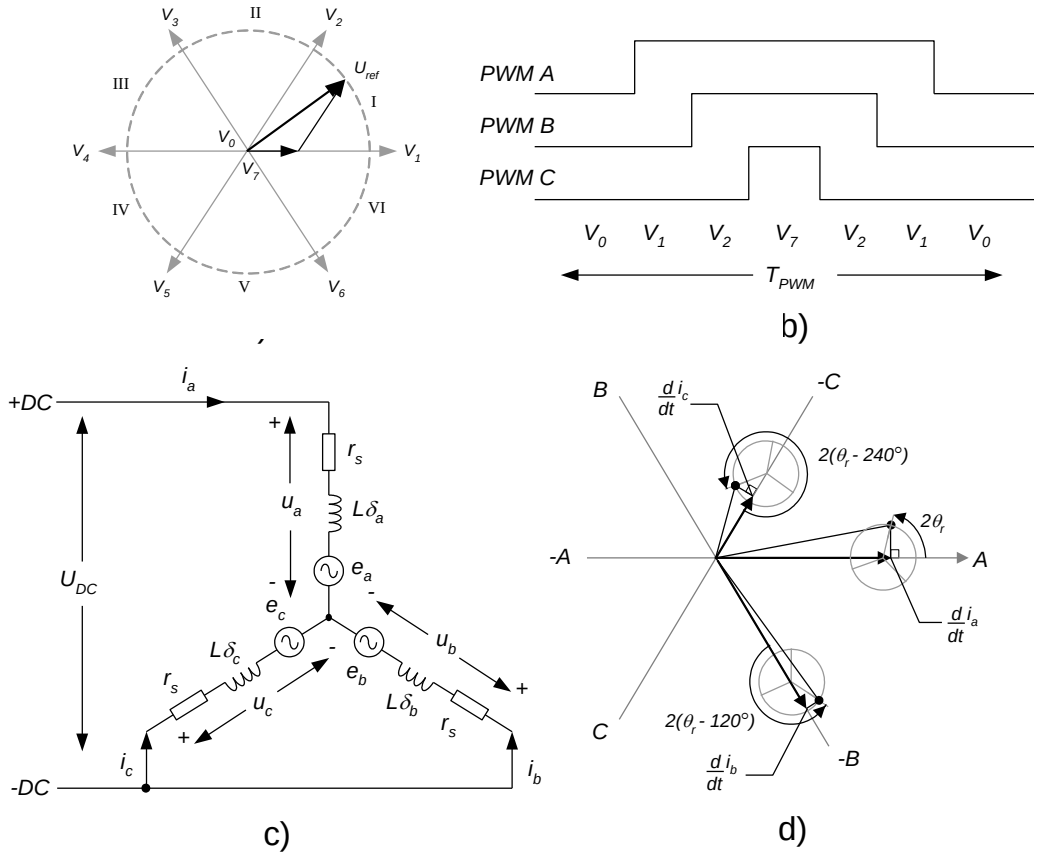

Figure 1. INFORM methodology; a) SVPWM modulation, b) switching sequence when u_{ref} is in sector I, c) Equivalent circuit for the PM machine, d) Current transient components under excitation of V_1

Ideally for each PWM cycle, two active vectors adjacent to the voltage reference vector and two null vectors are applied in sequence. Fig.1b shows the switching sequence for the case when u_{ref} is located in sector *I*, note that in this case the applied sequence is: $V_0 \rightarrow V_1 \rightarrow V_2 \rightarrow V_7 \rightarrow V_2 \rightarrow V_1 \rightarrow V_0$. Fig.1c shows the stator equivalent circuit for a start connected PM machine when V_1 is applied, where r_s is the stator resistance, e_{abc} are the back-EMF terms, u_{abc} are the phase voltages, and i_{abc} are the stator currents. Note that when V_1 is applied, the resulting current trajectories (derivatives) align to the phase voltage vector as that shown in Fig.1d. For any given rotor position the dominant saliency modulates the leakage inductances ($l_{\sigma a,\sigma b,\sigma c}$) which displaces the current vectors di_{abc}/dt along circular trajectories modulated by θ_{an} [28-29]. Similar current modulation as that shown in Fig.1 are expected for other vectors ($V_2 \ldots V_6$); the aim of INFORM is to estimate this displacement as a method not only to estimate the saliency position angle, but to assess the drive's condition.

2.1 Derivation of the INFORM approach

The analytical solution for INFORM can be described as follows: considering the case when V_1 is applied and considering the equivalent circuit of Fig.1a, expressions for the line to line voltages are obtained, which can be represented as:

$$\begin{aligned} U_{DC} &= \left(i_a^{(1)} r_s + l_{\sigma a}\frac{d}{dt} i_a^{(1)} + e_a\right) - \left(i_b^{(1)} r_s + l_{\sigma b}\frac{d}{dt} i_b^{(1)} + e_b\right) \\ -U_{DC} &= \left(i_c^{(1)} r_s + l_{\sigma c}\frac{d}{dt} i_c^{(1)} + e_c\right) - \left(i_a^{(1)} r_s + l_{\sigma a}\frac{d}{dt} i_a^{(1)} + e_a\right) \\ 0 &= \left(i_b^{(1)} r_s + l_{\sigma b}\frac{d}{dt} i_a^{(1)} + e_b\right) - \left(i_c^{(1)} r_s + l_{\sigma c}\frac{d}{dt} i_c^{(1)} + e_c\right) \end{aligned} \tag{2}$$

where the index "$^{(x)}$" is used to denote a current variable respect to an active vector (in this case V_1). Since the aim is to extract θ_{an} based on the current trajectories, it is evident from (2) that the resistive voltage drops and the back-EMF terms are not particularly useful. A practical way to remove them is by the application of an opposite vector [28-29] which in this case corresponds to V_4 (see Fig.1a); expressions for V_4 are:

$$\begin{aligned} -U_{DC} &= \left(i_a^{(4)} r_s + l_{\sigma a}\frac{d}{dt} i_a^{(4)} + e_a\right) - \left(i_b^{(4)} r_s + l_{\sigma b}\frac{d}{dt} i_b^{(4)} + e_b\right) \\ U_{DC} &= \left(i_c^{(4)} r_s + l_{\sigma c}\frac{d}{dt} i_c^{(4)} + e_c\right) - \left(i_a^{(4)} r_s + l_{\sigma a}\frac{d}{dt} i_a^{(4)} + e_a\right) \\ 0 &= \left(i_b^{(4)} r_s + l_{\sigma b}\frac{d}{dt} i_a^{(4)} + e_b\right) - \left(i_c^{(4)} r_s + l_{\sigma c}\frac{d}{dt} i_c^{(4)} + e_c\right) \end{aligned} \tag{3}$$

When combining (2) and (3) the following results:

$$\begin{aligned} 2U_{DC} &= l_{\sigma a}\left(\frac{d}{dt} i_a^{(1)} - \frac{d}{dt} i_a^{(4)}\right) - l_{\sigma b}\left(\frac{d}{dt} i_b^{(1)} - \frac{d}{dt} i_b^{(4)}\right) \\ 2U_{DC} &= l_{\sigma c}\left(\frac{d}{dt} i_c^{(1)} - \frac{d}{dt} i_c^{(4)}\right) - l_{\sigma a}\left(\frac{d}{dt} i_a^{(1)} - \frac{d}{dt} i_a^{(4)}\right) \\ 0 &= l_{\sigma b}\left(\frac{d}{dt} i_b^{(1)} - \frac{d}{dt} i_b^{(4)}\right) - l_{\sigma c}\left(\frac{d}{dt} i_c^{(1)} - \frac{d}{dt} i_c^{(4)}\right) \end{aligned} \tag{4}$$

As expected, the resistive voltage drops and the back-EMF terms have been removed which leaves an expression that is only dependant on the DC link voltage (a known variable), and the current trajectories [29]. Note that similar relations are expected for the remaining vectors (v_2-v_5) and (v_3-v_6). Since this is a star-connected machine, the next condition applies [29]:

$$\frac{d}{dt} i_a^{(k)} + \frac{d}{dt} i_b^{(k)} + \frac{d}{dt} i_c^{(k)} = 0, \text{ where } k = 1, 2\ldots, 6 \tag{5}$$

where *k* is an active vector number. By combining (4) and (5) an expression for the current trajectories for the opposite vectors V_1 and V_4 is obtained:

$$\frac{d}{dt} i_a^{(1)} - \frac{d}{dt} i_a^{(4)} = \frac{l_{\sigma b} + l_{\sigma c}}{l_{\sigma a} l_{\sigma b} + l_{\sigma b} l_{\sigma c} + l_{\sigma c} l_{\sigma a}} 2U_{DC} \tag{6}$$

By substituting (1) into (6), an expression containing information about θ_{an} is finally reached:

$$\frac{d}{dt}i_a^{(1)} - \frac{d}{dt}i_a^{(4)} = \frac{2}{g}\left(2 - \frac{\Delta l}{l_0}\cos(2\theta_{an})\right) \tag{7}$$

$$\text{with} \quad g = \frac{3l_0\left(1-\left(\frac{\Delta l}{2l_0}\right)^2\right)}{U_{DC}} \quad \text{as a constant value.} \tag{8}$$

Similar expressions are expected for the remaining vectors which are:

$$\begin{aligned}\frac{d}{dt}i_c^{(2)} - \frac{d}{dt}i_c^{(5)} &= \frac{2}{g}\left(2 - \frac{\Delta l}{l_0}\cos\left(2\left(\theta_{an} - \frac{4}{3}\pi\right)\right)\right)\\ \frac{d}{dt}i_b^{(3)} - \frac{d}{dt}i_b^{(6)} &= \frac{2}{g}\left(2 - \frac{\Delta l}{l_0}\cos\left(2\left(\theta_{an} - \frac{2}{3}\pi\right)\right)\right)\end{aligned} \tag{9}$$

Considering (1) and (7-9), general expressions related to the inductance modulation can be represented as:

$$\begin{aligned}L'_a &= \frac{\Delta l}{l_0}\cos 2(\theta_{an}) = 2 - \frac{g}{2}\left(\frac{d}{dt}i_a^{(1)} - \frac{d}{dt}i_a^{(4)}\right)\\ L'_b &= \frac{\Delta l}{l_0}\cos 2\left(\theta_{an} - \frac{2}{3}\pi\right) = 2 - \frac{g}{2}\left(\frac{d}{dt}i_b^{(3)} - \frac{d}{dt}i_b^{(6)}\right)\\ L'_c &= \frac{\Delta l}{l_0}\cos 2\left(\theta_{an} - \frac{4}{3}\pi\right) = 2 - \frac{g}{2}\left(\frac{d}{dt}i_c^{(2)} - \frac{d}{dt}i_c^{(5)}\right)\end{aligned} \tag{10}$$

where L_{abc}' can be considered as a measurement of phase leakage inductance l_σ, where the average value is represented by an offset value (+2), while the saliency modulation determined by θ_{an} depends exclusively from the current trajectories [28-29]. Since only the saliency modulation is relevant, Pos_{abc} can be represented as:

$$\begin{aligned}Pos_a &= \left(\frac{d}{dt}i_a^{(1)} - \frac{d}{dt}i_a^{(4)}\right)\\ Pos_b &= \left(\frac{d}{dt}i_b^{(3)} - \frac{d}{dt}i_b^{(6)}\right)\\ Pos_c &= \left(\frac{d}{dt}i_c^{(2)} - \frac{d}{dt}i_c^{(5)}\right)\end{aligned} \tag{11}$$

Considering that INFORM is aimed primarily as a method to estimate θ_{an}, Pos_{abc} is usually transformed into an orthogonal reference frame ($Pos_{\alpha\beta}$) which is obtained by (12), this way the information related to the saliency angle can be easily obtained from: $\theta_{an} = \tan^{-1}(Pos_\alpha/Pos_\beta)$. The health condition will be assessed from (12) as it will be demonstrated in the next sections.

$$\begin{aligned}Pos_\alpha &= \left(\frac{d}{dt}i_a^{(1)} - \frac{d}{dt}i_a^{(4)}\right) - \frac{1}{2}\left(\left(\frac{d}{dt}i_b^{(3)} - \frac{d}{dt}i_b^{(6)}\right) + \left(\frac{d}{dt}i_c^{(2)} - \frac{d}{dt}i_c^{(5)}\right)\right)\\ Pos_\beta &= -\frac{\sqrt{3}}{2}\left(\left(\frac{d}{dt}i_b^{(3)} - \frac{d}{dt}i_b^{(6)}\right) - \left(\frac{d}{dt}i_c^{(2)} - \frac{d}{dt}i_c^{(5)}\right)\right)\end{aligned} \tag{12}$$

2.2 Implementation of the INFORM algorithm

As described before, a relationship between the current trajectories and the saliency characteristics can be extracted by the application of a series of vectors which are aimed to remove the influence of resistive voltage drops and back-EMF terms [28-29]. These vectors consist of a sequence of short duration pulses where direct and opposite vectors ($V_1 \rightarrow V_4$, $V_3 \rightarrow V_6$, $V_5 \rightarrow V_2$) are applied in sequence during the inactive state (V_7). After each vector is applied, a sampling for the phase current trajectories (di/dt) are required which will be used to built the saliency modulation components according to (12). This approach is represented in Fig.2 for the case of three consecutive PWM switching periods for the case when u_{ref} is located in sector *I*.

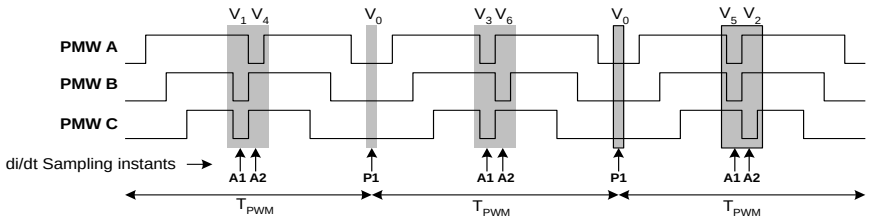

Figure 2. INFORM method: PWM sequence when u_{ref} is in the switching sector I

In this basic form, INFORM requires three samples per PWM cycle to monitor the currents response. These instants are indicated by arrows and can be described as follow: samples A_1 and A_2 are taken after the application of the basic vectors, which are applied in the middle of the inactive state V_7; this to avoid disruption of the average voltage [29] supplied. An additional sample denominated as P_1 is required which is applied in the middle of the inactive state V_0. The process is repeated for other switching sectors according to the location of u_{ref} [29]. Fig.3 shows the relevant components required by INFORM to extract the saliency information: the current measurements are shown in Fig.3a, followed by the phase current trajectories (d/dt measurements) which were obtained during instants A_1, A_2 and P_1 according to the PWM sequence (see Fig.3e). The constructed three-phase (11) and $\alpha\beta$-frame saliency (12) are shown at Fig.3f and Fig.3g respectively. It should be stated that units of y-axis in the last two graphs of Fig.3 is related to instantaneous rate of current change (amps/sec) since the saliency characteristics where obtained from several portions of di/dt measurements.

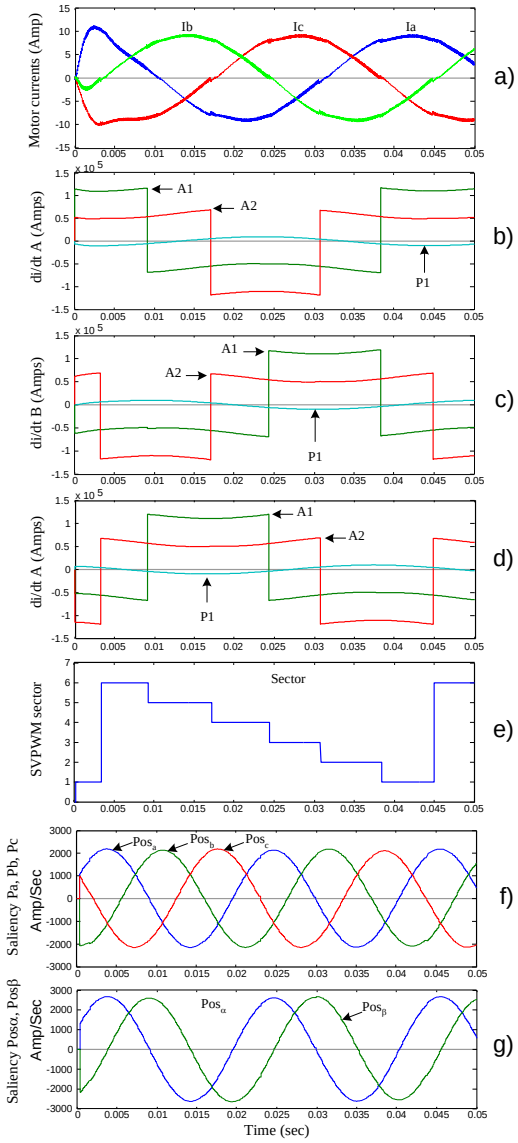

Figure 3. INFORM method, calculation of the saliency components: a) Motor currents; b), c), d) *di*/*dt* measurements for A_1, A_2 and P_1 instants; e) PWM sectors; f) three-phase saliency; g) αβ-frame saliency.

III. SALIENCY MODULATION PROFILE (SMP)

The Saliency Modulation Profile (SMP) concept was initially proposed to improve the rotor position estimation in sensorless control applications [20-21]. Later, the scheme was modified and combined with saliency tracking to allow high performance in saliency-based condition monitoring [18]. SMP can be considered as the electromagnetic signature of a drive operating under healthy conditions and will be used to monitor changes in performance due to the presence of faults. This profile is obtained during commissioning and is stored in a lookup table for later use. Fig.4a shows the SMP for the machine considered in this study. As observed SMP can be represented as two surfaces (Pos_α* and Pos_β*), where the saliency information is determined according to two variables: the mechanical angle (θ_r), and the load torque level (determined by I_q* from the controller) [18]. The procedure to calculate the SMP is represented in Fig.4b and can be summarized as follows:

the shaft is rotated at low constant speed, while $Pos_{\alpha\beta}$ measurements are obtained according to (12). A band-pass filter (non-casual) tuned at the corresponding saliency frequency which is determined by the rotor speed and rotor pole pairs, is used to remove any distortions from measurements [30]. The filtered signals are averaged

considering an integer number of mechanical revolutions to guarantee accuracy (a minimum of three rotations was considered in this work). Finally, the averaged values are stored in lookup tables as function of the rotor position angle. In this work, a single rotation was divided into 256 discrete intervals to maintain accuracy in a compact lookup table. The procedure is repeated for several loads to cover all expected conditions. Interpolation between loads is allowed to increase accuracy of the profile by increasing the number of sampled points [30].

The process to determine the condition of the drive is summarised in Fig.4c: the scheme compares the measured saliency ($Pos_{\alpha\beta}$) against the "healthy saliency" ($Pos_{\alpha\beta}$*) obtained from the lookup tables according to θ_r and I_q*.

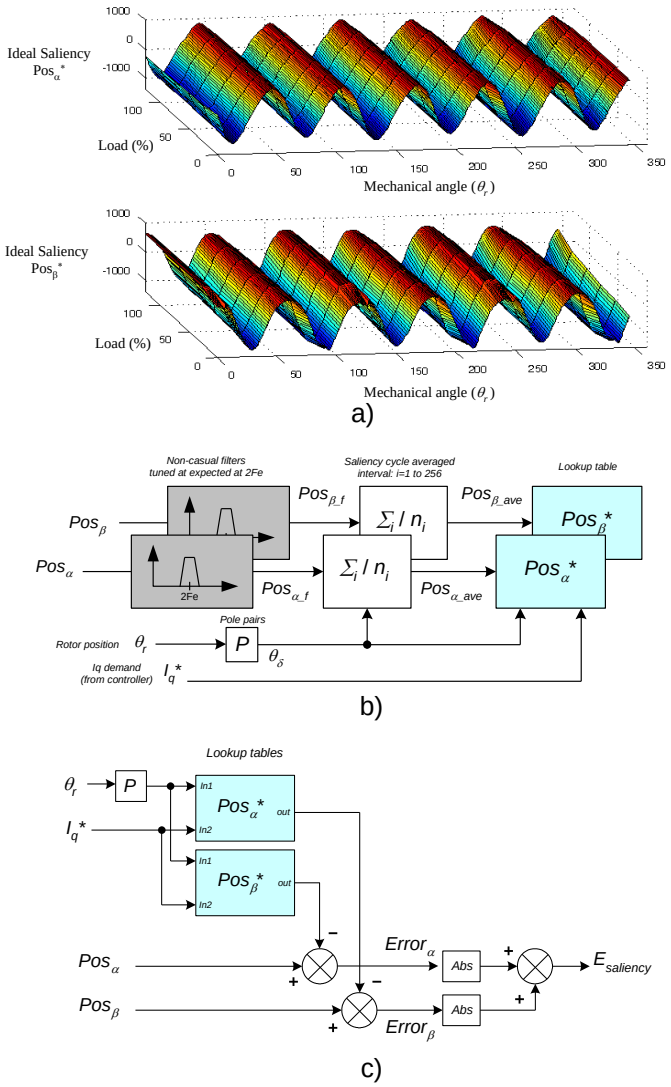

Figure 4. SMP approach: a) Electromagnetic profile for the machine considered; b) Schematic diagram for calculation of the SMP tables; c) Detection of the drive's condition by $E_{saliency}$

A relevant aspect is that $Pos_{\alpha\beta}$* is independent of the rotor speed, therefore the only parameter to consider during their construction is the torque level (determined by I_q*) [30]. From Fig.4c, note that the absolute value for the differences between $Pos_{\alpha\beta}$ and $Pos_{\alpha\beta}$* are used to calculate a new variable denominated as $E_{saliency}$ which is used to trigger warnings or alarms [18] as faults develop. It is clear that when system is operating under healthy conditions $E_{saliency}$ will be very close to zero and will change significantly in the presence of faults accordingly to the severity of a fault.

3.1 Considerations for implementation

For the experimental system used in this work, duration of the excitation pulses is 8μsec which is long enough to allow the power devices to supply the excitation voltage accurately (in this case the IGBT devices used have a turn-on time of 70nsec, and turn-off time of 400nsec). In practice high distortions for the *d*/*dt* measurements are expected due to unwanted oscillations after the applications of the testing vectors [23]. A simple way to reduce their impact is to use *di*/*dt* sensors instead of calculating the derivative values between two consecutive samples. For the approach implemented in this work, Rogowski coil sensors and physical low-pass filters tuned at a cutting frequency of 250kHz were selected to clean out the current trajectories [29]. These actions are not usually sufficient to remove all distortions from the *d*/*dt* measurements; therefore a short delay (waiting period) is required to allow dissipation of the residual energy before sampling. For this work, a waiting delay of 5μsec was found sufficient to guarantee high quality estimation [29] which is updated every 100msec.

Relevant aspects to consider for the practical implementation is that INFORM requires specific hardware capabilities; for instance the INFORM cycle interrupts the normal PWM pattern in order to apply the required excitation vectors. Further, the scheme requires sampling triggered by the edges of the PWM voltages rather than conventional synchronous sampling. These characteristics can only be achieved by powerful processing platforms offering high flexibility in PWM generation and sampling. For the experimental system used in this work, a DSP-FPGA embedded platform was used [29]. This architecture releases the DSP from heavy processing load which increases availability for complex tasks. Fortunately similar architectures can be found in modern high-systems drives which may help to facilitate adoption of INFORM not only for sensorless operation, but for condition monitoring purposes.

Respect to the SMP approach, it is recognized that generation of the saliency lookup tables may be difficult and impractical for certain applications; however since the INFORM method is not sensible to the inverter nonlinearities, the stored saliency ($Pos_{\alpha\beta}$*) depends exclusively from the machine which ensures very similar SMP tables for identical machines produced by the same manufacturer. This assumes that the SMP tables could be obtained directly from the manufacturer, or obtained by the user during commissioning once to be stored, so could be used for all drives based on the considered machine. Note that the SMP profiles are valid for one single value of the magnetizing current which is usually maintained to zero (I_d*=0); however if field-weakening region is required, different lookup tables will be required which may increase complexity of the approach.

IV. Evaluation of PWM Transient Exitation in the Precense of Winding Faults

This section contains numerical and experimental evaluations for the case of a PMSM drive subjected to the presence of two types of winding faults: *short circuits* and *incipient insulation faults*. The evaluated machine is a 6-pole 3.82kW surface mounted PM motor (shown in Fig.5), which has links to the stator windings brought out, so different combinations of faults can be implemented. A finite element (FE) representation for the considered machine was also developed (shown in Fig.5b) to validate the experimental findings numerically. The relevant parameters and characteristics of the machine are contained in the Appendix.

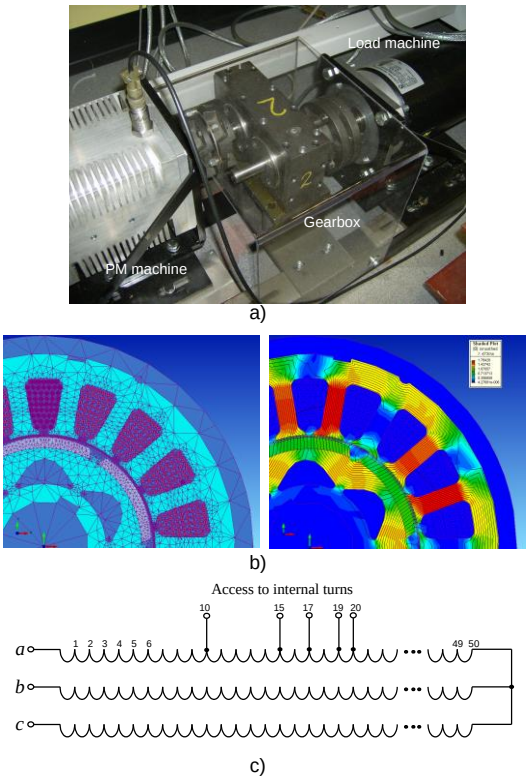

Figure 5. Evaluated machine; a) Experimental system, b) FE motor model, c) Winding connections

4.1 Numerical evaluation

A co-simulation between FE-software (MagNet) and Matlab/Simulink was implemented to evaluate the monitoring approach numerically. In this case, the vector control algorithm, the INFORM approach, and SMP were implemented on Simulink, while a detailed FE model of the machine was implemented for a realistic drive representation. The performance of the saliency-based monitoring approach shown in Fig.4c is evaluated here in the presence of inter-turn short circuit faults of several magnitudes. The cases considered are: one, two, five and ten inter-turn short circuits. The resulting for the saliency error parameter ($E_{saliency}$) is shown in Fig.6 when the machine is operated at 600RPM (in this case the fundamental frequency applied is 30 Hz), while the load is maintained to 50% the nominal value.

One can observe from Fig.6a that when the drive is operating under healthy conditions ($t < 15mSec$), $E_{saliency}$ is very close to zero as expected, and changes considerably when a fault is applied ($t > 15mSec$). It is clear that the average value of $E_{saliency}$ increases as the number of affected turns is also increased which confirms that $E_{saliency}$ can be used not only to detect the presence of a fault, but to determine its magnitude respect to a healthy system. Note that for the case of 10-turns fault, $E_{saliency}$ increases in magnitude every period. This is because the 10-turn fault produces a significant unbalance (the total number of turns per coil is 50). This unbalance introduces torque oscillations which affects speed. The increments observed are effects of the speed loop trying to compensate the oscillations by slowly increasing the I_q demand. Fig.6b shows $E_{saliency}$ respect to the electrical angle (Loci plot). This plot is particularly interesting since can be used to detect the type of fault and its location within the stator windings [18].

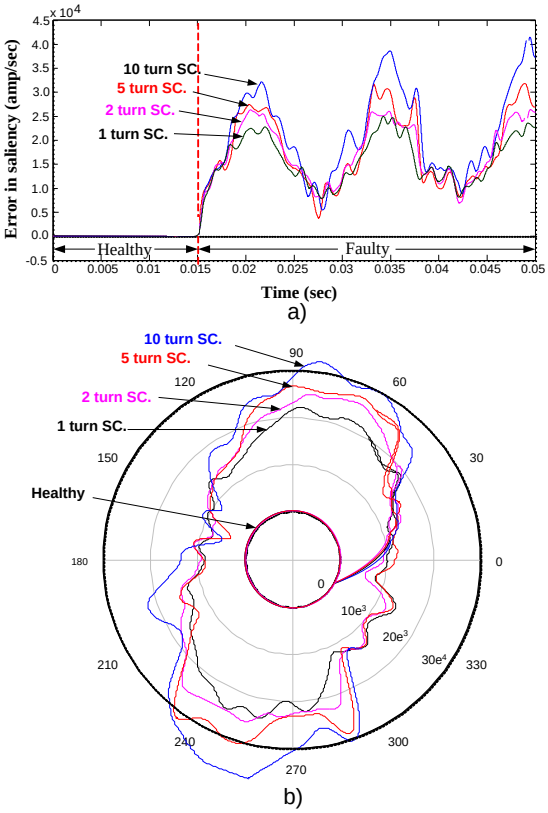

Figure 6. Numerical evaluation; faults considered: 1, 2, 5 & 10 inter-turn short circuits; a) $E_{saliency}$ respect to time, b) $E_{saliency}$ respect to the electrical angle (Loci plot).

4.2 Experimental Evaluation

This section contains experimental results for the PMSM drive (shown in Fig.5a) which is subjected to the presence of several winding faults. Two types of faults are considered: inter-turn short circuits (evaluated numerically in the previous subjection), and incipient insulation degradation faults. Evaluation of the scheme is first considered in the presence of a full short-circuits which is shown in Fig.7. For this test the machine is operated at 600RPM (supplied frequency F_e=30 Hz) with a load of 50% of the nominal value. Figs.7a-b show a comparison between $Pos_{\alpha\beta}$ (online saliency) and $Pos_{\alpha\beta}$* (lookup table) under two conditions: healthy and faulty operation; in this case the evaluated fault consists of one turn short circuit applied @ t = 25$mSec$ to the coil of phase A. Note that $Pos_{\alpha\beta}$ is very close to $Pos_{\alpha\beta}$* when the drive is operating under healthy conditions (the small differences are due to errors and noise picked up during measurement), while a significant variation in saliency is observed when the fault is applied. Note that in this case a significant variation in Pos_{α} is observed respect to Pos_{β} which is hardly affected. This is because of the location of the fault which in this case was applied to a coil of phase A; however significant variations in Pos_{β} would be expected for other faults located in phases B and C of the stator windings. The saliency errors between $Pos_{\alpha\beta}$ and $Pos_{\alpha\beta}$* are represented in Fig.7c, while $E_{saliency}$ is shown in Fig.7d. The variation of $E_{saliency}$ in the presence of the fault (one turn short circuit) is evident. Note the quick response of the scheme (less than 2$mSec$); this is vital to avoid further damage assuming that proper corrective actions are implemented once a warning has been trigged by $E_{saliency}$.

The monitoring scheme is further evaluated in the presence of inter-turn full short circuits and the presence of incipient faults. Insulation degradation is modelled here by the connection of a small value resistor between the affected turns (1.0Ω is used in this work).

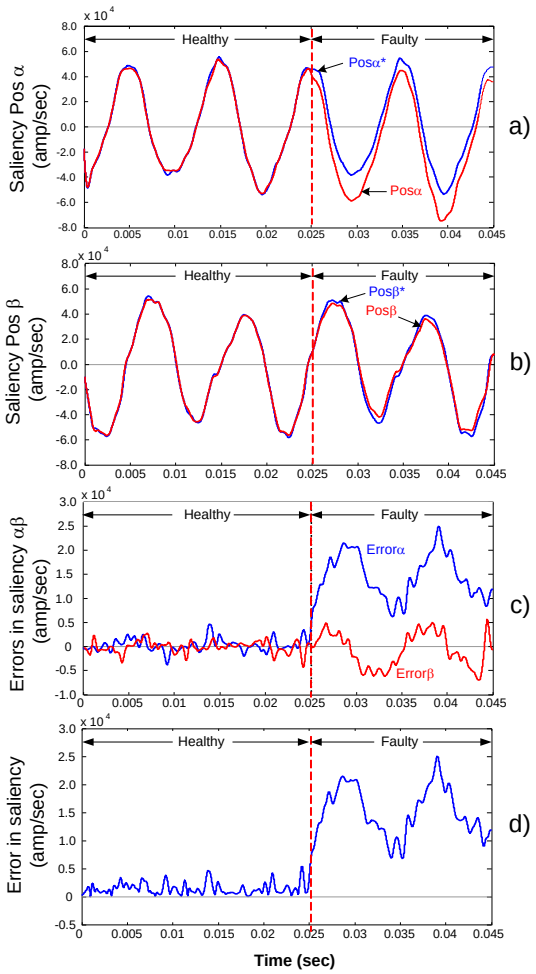

Figure 7. Experimental evaluation; transition between a healthy to a faulty drive (one-turn short circuit applied): a-b) saliency components $Pos_{\alpha\beta}$; c) $\alpha\beta$-errors; d) Error in saliency $E_{saliency}$

A comparison between full short circuits and incipient winding faults considering the same number of affected turns (faults applied to a coil of phase *A*) is shown in Fig.8; the left side graph shows the response for inter-turn full short circuits, while graph at the rigth side shows the case of incipient winding faults. A comparison for the system operating under healthy conditions is included for comparison purposes.

The faults considered (full short circuits and incipient faults) consist of several magnitudes: one, three, and five turns. Note that in this test the machine is operated at low speed range (30 RPM) to limit the amount of induced current in the affected turns while the load is maintained at 50% of the nominal value. Note that for the case of a healthy system, $E_{saliency}$ remains close to zero as expected (Figs.8a-b). The small differences observed are due to noise picked up during measurement and other saliencies not considered by the SMP scheme. For the case of a faulty system (1, 3 and 5 inter-turn faults), note that $E_{saliency}$ changes considerably respect to a healthy system. It is clear that $E_{saliency}$ is very sensitive for all faults considered, even in the case for the smallest fault which corresponds to *one-turn incipient* winding fault (this condition is represented in the red in Fig.8b). Note that the equivalent *one-turn full short circuit* fault (represented in red in Fig.8a) shows a higher increment in $E_{saliency}$ which provides an indication of a bigger fault. Similar situation is observed for the other magnitude considered (three and five inter-turn faults). According to Fig.8, it is clear that $E_{saliency}$ can be used to give an indication of the severity and type of a fault. Big variations are expected for full short circuits, while small changes are related to incipient faults.

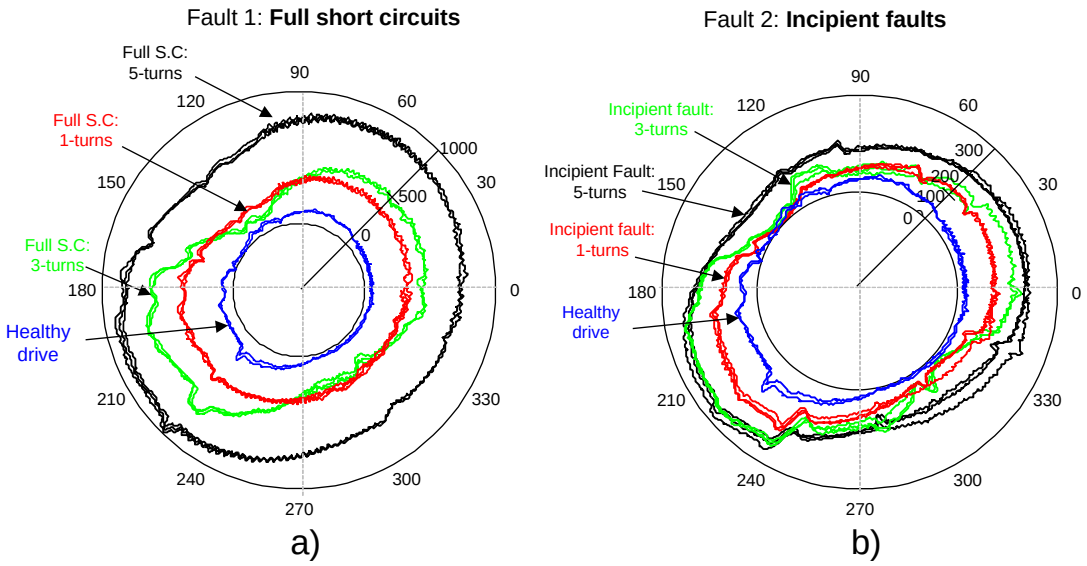

Figure 8. Experimental evaluation between full-short circuits and insulation degradation faults: Comparison between a healthy, and faulty system (1, 3, & 5 turns affected); a) Full short circuits, b) Incipient faults.

As a final test, the proposed scheme is evaluted under standstill operation (a position controller is implemented); in this case the rotor is maintained to a fixed position (0° mechanical), while a load of 50% is applied. Results for the phase saliency (Pos_{abc}) and the saliency error ($E_{saliency}$) are represented in Fig.9. The transition from a healthy to a faulty operation is investigated in order to evaluate the performance of scheme. In this case the applied fault consists of 3-turn full short circuits suddenly applied at t=0.9sec.

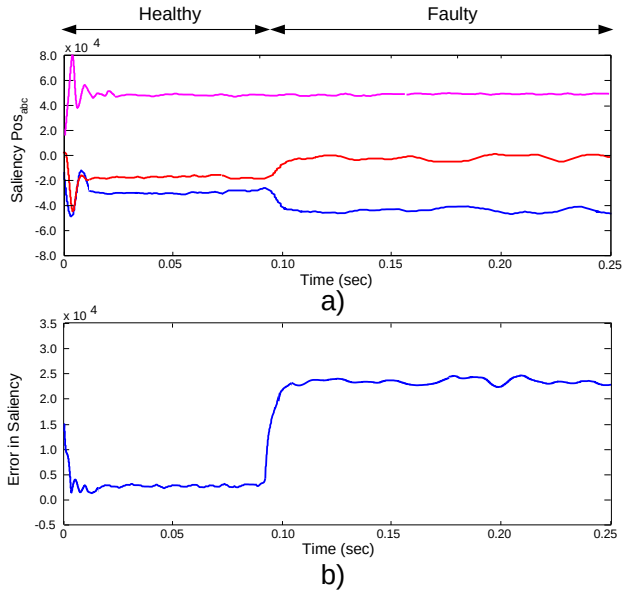

Figure 9: Evaluation under standstill operation, transition between a healthy to faulty system; a) Position estimates (Pos_{abc}); b) Error in saliency $E_{saliency}$

Note that the position estimates remain close to a fixed value after some initial transients resulting from the INFORM method activated at t=0sec. Since in this case the machine is initially operated under healthy conditions the resulting $E_{saliency}$ (see Fig.9b) remains very close to zero as expected. Note that in this case the fault was applied to phase B which produces significant variations in Pos_b and Pos_c; while Pos_a remains unaffected. A significant variation in $E_{saliency}$ is observed when the fault is applied; this confirms that the proposed scheme is suitable also for standstill operation which makes it ideal for position control applications.

V. CONCLUSIONS

The monitoring scheme presented in this paper is an improved version of the HF-injection based condition monitoring scheme previously developed by these authors. In this case, the INFORM methodology is selected to assesses the drive condition since the approach has relevant advantages. For instance, INFORM has no speed-range restrictions which make it suitable for virtually any sensored/sensorless drive applications. Further, the INFORM is insensitive to the inverter nonlinearities which increase the detection capabilities further. A relevant aspect is that proposed scheme has the capability to assess the drive's condition under standstill operation; this means that the approach is suitable for position control applications.

The presented approach determines the condition of the drive by comparing the extracted saliency (which is considerable affected in the presence of electromagnetic faults) against the magnetic signature from a drive operating under healthy conditions. The obtained difference is used to trigger warnings or alarms that can be used to avoid further degradation. The result in a monitoring scheme that is able to detect faults that would be particularly difficult to evaluate under nonstationary conditions; that is the case of incipient winding faults, or the presence of inter-turn short circuits (both scenarios have been extensively investigated in this work).

The simulation and experimental results presented confirm quick response, and remarkable detection capabilities. The presented results validate the performance of the scheme not only in the detection of a fault, but to determine its magnitude. The proposed scheme can be easily integrated as part of the drive's own safety features in sensorless applications based on the INFORM topology.

APPENDIX

ELECTRICAL PARAMETERS FOR THE PM MACHINE

Number of poles:	6
Type of magnets:	Surface mounted
Number of stator slots:	18
Turns per coil:	50
Rated speed:	3000 (rpm)
Rated torque:	12.2 (Nm)
Rated power:	3.82 (kW)
Kt:	1.6 (Nm/A)
Ke:	98.0 (Vrms/krpm)
Inertia:	20.5 ($kgcm^2$)
R (ph-ph):	0.94Ω
L (ph-ph):	8.3mH

REFERENCES

[1] Motor reliability working group. "Report of large motor reliability survey of industrial and commercial installations, Part I," *IEEE Trans. Ind. Appl*., vol. IA-21, No. 4, pp: 853-864, Jul. 1985.

[2] Motor reliability working group. "Report of large motor reliability survey of industrial and commercial installations, Part II," *IEEE Trans. Ind. Appl*., vol. IA-21, No. 4, pp: 865-872, Jul. 1985.

[3] O. V. Thorsen, M. Dalva; "A survey of faults on induction motors in offshore oil industry, petrochemical industry, gas terminals, and oil refineries; *IEEE Trans. Ind. Appl*., Vol. 31, No. 5, pp: 1186-1196, Sep./Oct. 1995.

[4] D. E. Shump, "Testing to assure reliable operation of electrical motors," in *Proc. IEEE Ind. Appl. Soc. 37th Annu. Petrol. Chem. Ind. Conf*., Sep. 1990, pp: 179-184.

[5] S. Grubic, J. M. Aller, B Lu, T. G. Habetler; "A surcey on testing and monitoring methods for stator insulation systems of low-voltage induction mechines focsusing on turn insulation problems," *IEEE Trans. Ind. Elect*., Vol. 55, No. 12, pp: 4127-4136; Dec. 2008.

[6] G. C. Stone, E. A. Boulter, I. Culbert, H. Dhirani, *Electrical insulation for rotating machines: design, evaluation, aging, testing and repair*; Piscataway, NJ: IEEE Press, 2004.

[7] S. B. Lee, R. M. Tallam, T. G. Habetler, "A robust on-line turn-fault detection technique for induction machines base on monitoring the sequence component impedance matrix," *IEEE Trans. Power Electron*., Vol. 18, No. 3, pp: 865-872, May 2003.

[8] M. Arkan, D. K. Perovic, P. Unsworth, "Online stator fault diagnosis in induction motors," in *Proc. Ins. Elect. Eng.-Elect Power Appl*.; Vol. 148, No. 6, pp. 537-547, Nov. 2001.

[9] M. A. Cash, T. G. Habetler, G. B. Kliman, "Insulation failure prediction in AC machines using line-neutral voltages," *IEEE Trans. Ind. Appl*., Vol. 34, No. 6, pp.1234-1239, Nov./Dec. 1998.

[10] A. Babel, A. Muetze, R. Seebacher, K. Krischan, E. G. Stangas, "Inverter device nonlinearity characterization technique for use in a motor drive system," *IEEE Appl. Power Electron. Conf and Expos. APEC 2014*; pp:2767-2774; 2014.

[11] J. H. Hung, J. J. Lee, B. H. Kwon; "Online diagnosis of induction motors using MCSA,"in *IEEE Trans. Ind. Electron*., Vol. 53, No. 6 pp: 1842-1852; Dec. 2006.

[12] F. C. Trutt, J. Sottie, J. L. Kohler, "Condition monitoring of induction motors stator winding using electrically excited vibrations," in *Conf. Rec. 37th IEEE IAS Annu. Meeting*; Vol. 4, pp: 2301-2305; Oct. 2002

[13] T. Assat, H Henao, G. A. Capolino, "Simplified axial flux expectrum method to detect incipient stator inter-turn short-circuits in induction machine," in *Proc. IEEE Int. Symp. Ind Electron*.; Vol. 2, pp; 815-819; May. 2004.

[14] Z. Chen, R. Oi, H. Lin, "Inter-turn short circuit fault diagnosis form PMSM based on complex gauss wavelet"; *IEEE Int. Conf. on Wavelet. Analysis and pattern recognition*; pp.1915-1919; Nov. 2007.

[15] B. Aubert, J. Regnier, S. Caux, D. Alejo; "Stator inter-turn short-circuit detection in permanent magnet synchronous generators using extended Kalman filtering"; in *Proc. IEEE Int. Works. of Elect. Meas. Sign. and their App. to Mech; ECMSM'2013*; pp:1-6; 2013.

[16] P. Werynski, D. Roger, R. Corton, J. F. Brudny, "Proportion of a new method for in-service monitoring of the aging of stator winding insulation in AC motors," *IEEE Trans. Energy Convers*., Vol. 21, No. 3, pp: 673-681; Sep. 2006.

[17] F. Briz, M. W. Degner, A. B. Diez, J. M. Guerrero; "Online diagnostics in inverter-fed induction machines using high-frequency signal injection," *IEEE Trans on Ind. Applic*., Vol. 40, No. 4; pp. 1153-1161; July/August 2004.

[18] J. Arellano-Padilla, M. Sumner and C. Gerada, "Winding condition monitoring scheme for a PM machine by using HF injection," *IET Electric Power Applic. Journal*; Vol. 5, Issue 1, pp. 89-99; 2011.

[19] W. Limei, R. D. Lorenz; "Rotor estimation for permanent magnet synchronous motor using saliency-tracking self-sensing method"; *IEEE Ind. Applic. Conf*.; Vol. 1, pp: 445-450, year: 2000.

[20] N. Teske, G. Asher, M Sumner, K. J. Bradley; "Analysis and suppression of high-frequency inverter modulation in sensorless position-controlled induction machine drives"; *IEEE Trans. Ind. Applic*. Vol.39, Issue: 1, pp. 10-18, 2003.

[21] C. A. Silva, G. M. Asher, M. Sumner and K. J. Bradley, "Sensorless rotor position control in a surface mounted PM machine using HF voltage injection," in *Proc. EPE-PEMC'02*; year: 2002.

[22] T. M. Wolbank, M. K. Metwally; "Comparison of inherent saliency tracking methods for zero speed sensorless control of standard induction machines"; *IEMDC'09 conference*; pp: 1258-1263; Year: 2009.

[23] M. Schroedl, "Sensorless control of AC machines at low speed and standstill based on the INFORM method," in *Conf. Rec. IEEE Annu. meeting*, vol.1, pp.270-277; year: 1996.

[24] E. Robeischl, M. Schroedl, "Optimized INFORM measurement sequence for sensorless PM synchronous motor drives with respect to minimum current distortion"; *IEEE Transaction of industry applications*," Vol.40, pp.591-598, Mar/April 2004.

[25] 7 P.L. Jansen, and R.D. Lorenz, "Transducerless position and velocity estimation in induction and salient AC machines," *IEEE Trans. Ind. Applicat*., Vol: 31, Issue: 2, pp: 240-247; Year: 1995.

[26] S. C. Yang, T. Suzuki, R. D. Lorenz, T. M. Jahns; "Surface-permanent-magnet synchronous machine design for saliency tracking self-sensing position estimation at zero and low speeds"; *IEEE Trans. on Ind. Applic*. Vol.47, Issue: 5; pp. 2103-2116, Year: 2011.

[27] P. G. Handley, J. T. Boys, "Space vector modulation: an engineering review"; in *Proc. 4th International conference on power electronics and variable speed drives*; London, UK; pp:87-91; Jul 1991.

[28] P. Nussbaumer; T. M. Wolbank; "Saliency tracking based sensorless control of AC machines exploiting inverter switching transients"; in *Proc. Conf. SLED 2010*; pp:114-119; Year:2010.

[29] H. Yahan, "Sensorless control of surfaced permanent magnet machine using fundamental PWM excitation," in *PhD. Thesis, University of Nottingham*, 2009.

[30] 17 C. A. Silva, "Sensorless vector control of Surface mounted permanent magnet machines without restriction of zero frequency," in *PhD. Thesis, University of Nottingham*, 2003.